



CHORUS

This is the accepted manuscript made available via CHORUS. The article has been published as:

Systematics of black hole binary inspiral kicks and the slowness approximation

Richard H. Price, Gaurav Khanna, and Scott A. Hughes

Phys. Rev. D **83**, 124002 — Published 1 June 2011

DOI: [10.1103/PhysRevD.83.124002](https://doi.org/10.1103/PhysRevD.83.124002)

Systematics of black hole binary inspiral kicks and the slowness approximation

Richard H. Price

*Department of Physics & Astronomy and CGWA,
University of Texas at Brownsville, Brownsville TX 78520*

Gaurav Khanna

Department of Physics, University of Massachusetts, Dartmouth, MA 02747

Scott A. Hughes

*Department of Physics and MIT Kavli Institute,
MIT, 77 Massachusetts Ave., Cambridge, MA 02139*

During the inspiral and merger of black holes, the interaction of gravitational wave multipoles carries linear momentum away, thereby providing an astrophysically important recoil, or “kick” to the system and to the final black hole remnant. It has been found that linear momentum during the last stage (quasinormal ringing) of the collapse tends to provide an “antikick” that in some cases cancels almost all the kick from the earlier (quasicircular inspiral) emission. We show here that this cancellation is not due to peculiarities of gravitational waves, black holes, or interacting multipoles, but simply to the fact that the rotating flux of momentum changes its intensity slowly. We show furthermore that an understanding of the systematics of the emission allows good estimates of the net kick for numerical simulations started at fairly late times, and is useful for understanding qualitatively what kinds of systems provide large and small net kicks.

I. INTRODUCTION

Since the breakthrough work by Pretorius[1], and by the Brownsville and Goddard groups[2, 3], numerical relativity (NR) has developed to the point that at present there are few limitations, except computer time, on the modeling of the inspiral of binary black holes. Among other phenomena that can now be studied numerically is the linear momentum contained in the gravitational waves emitted during inspiral. The result of this emission of momentum is the recoil of the final merged black hole, with significant consequences for scenarios of galactic evolution and electromagnetic signals from the effect of the recoil on the merged remnant’s environment. See, for example, Refs. [4–8] for recent work discussing astrophysical implications of black hole kicks.

The process of inspiral/merger can be divided into an early slow quasicircular inspiral, driven by gravitational wave radiation reaction, and late quasinormal ringing at complex frequencies characteristic of the spacetime of the final hole. The transition between the two different regimes is often called the plunge.

Schnittman et al. [9] seem to have been the first to notice that NR results show a general tendency for the radiation of linear momentum to reverse direction (although this result had been predicted about a year earlier by Damour and Gopakumar[10]). In deconstructing the computations of collisions of comparable mass holes Schnittman et al. found that some of the pre-plunge “kick” provided by the early quasicircular inspiral is canceled by a large “antikick” during the post-plunge quasinormal ringing. This “antikick” can be drastic. For one of the models studied by Schnittman et al. the final total kick was only around one third of the maximum kick, a maximum that occurs around the start of the binary plunge.

Particle perturbation methods[11, 12], with their relative simplicity, provide an important tool for probing points of principle, such as the antikick cancellation, more efficiently than full NR. Such modeling[11] has shown that for appropriate binary parameters (equatorial orbits, rapidly spinning background hole) the cancellation can be almost total. A cancellation of 97% of the maximum linear momentum was found for an equatorial inspiral for background spin parameter $a/M = 0.9$, and mass ratio 10^{-4} [13]. (The mass ratio is relevant since it governs the rate at which the quasicircular pre-plunge orbits decay.)

Attempts to understand this cancellation have led to a focus on the multipole structure of the gravitational wave emission[9, 11]. A single multipole carries no linear momentum.

It is the interaction of modes that gives rise to net linear momentum. The radiation in the $z = 0$ plane, for example, can carry linear momentum only if the radiation contains modes with both even and odd azimuthal indices m . The linear momentum, furthermore, is sensitive to the relative phase of the multipoles. While this multipole analysis is important it has not seemed to give a satisfactory answer to the underlying question: what can it be in the conditions of the pre-plunge radiation or motion, that “sets up” a plunge and ringdown that provide an antikick that almost cancels the initial kick? Some interesting underlying mechanisms have been proposed[14].

We will show here that in fact the phenomenon of antikick cancellation has nothing that is specific to gravitational radiation, to black holes, or to mixtures of multipoles. Rather, it is a general consequence of the way in which the radiation gradually builds up in time, and then dies off in a way that is in some sense gradual. Here “gradual” means that the oscillatory period of the radiation is short compared to the timescale for the change in the intensity and period of the radiation. It turns out that this condition is not strictly obeyed during the plunge, and that the condition is in fact quite difficult to define, and may ultimately have to be accepted as a qualitative criterion. Nevertheless it will be clear that this is the basic feature of the radiation that accounts for the strong antikicks.

As already mentioned, the prediction of an antikick had already been made in 2006 by Damour and Gopakumar[10]. In attempting to apply the effective one body approximation to kick calculations they pointed to the importance of the ratio of the orbital period to the timescale. It is particularly interesting that they identified (as do we) the epoch of the plunge as the crucial time for determining the net kick, and found that its details were crucial and not amenable to their approximations. These conclusions are all very similar to our own, though from a rather different point of view.

The phenomenon of the antikick, furthermore, is very robust. It applies just as well to nonlinear models as to linearized models. This general insight, furthermore, gives an immediate understanding of the conditions – at least the qualitative conditions – under which the antikick will give a significant reduction in recoil, and when the antikick can be ignored. In addition, this insight provides a possible efficiency in the computation of kicks. It shows that a binary model can be started very late, i.e., not long before the plunge, and yet yield a good estimate of the linear momentum radiated.

In this paper we present an analysis confined to equatorial binary orbits (i.e., for holes

whose spin, if nonzero, is perpendicular to the orbital plane). These are the cases in which the antikick can be dramatically strong. We will comment only briefly and speculatively on the extension of our analysis to more general configurations.

The remainder of this paper is organized as follows. In Sec. II we start by giving an analysis based on a “slow approximation.” We introduce a simple toy model with a well defined time scale for change, and we show that this model duplicates the behavior found in gravitational radiation. We then show that for gravitational radiation computational results there is a correlation between the “slowness” of the inspiral/merger and the extent of the antikick cancellation of the kick, but that it is difficult to make the correlation quantitative. In Sec. III, we show a very different side of the slow approximation; we demonstrate that based on this approximation, a good estimate of the radiated momentum can be found from a computation started shortly before the plunge. We summarize in Sec. IV and discuss possible extensions of this work.

II. KICK-ANTIKICK CANCELLATION FOR QUASICIRCULAR EQUATORIAL ORBITS

A. General analysis

We start by considering two objects in quasicircular orbits around each other in such a way that there is a symmetry of all physical features with respect to the orbital plane, so that linear momentum flux must be parallel to the orbital plane. The binary system could be a point particle orbiting in the equatorial plane of a Kerr hole or two comparable mass objects (black holes or stars) with their spin axes perpendicular to the orbital plane.

We use inertial Cartesian coordinates to describe the spacetime far from the orbiting bodies, with the orbital-symmetry plane taken to be the xy plane, and the system supposed to have its orbital angular velocity in the positive z direction.

In general, the orbital frequency $\Omega(t)$ will be a slowly changing function of time, and the rate of emission of linear momentum, which we will denote $f(t)$, will be a function of time due to the changing frequency and radius of the motion. Here all physical quantities, the linear momentum, the frequency, and the time t , are understood to be measured in the asymptotically flat spacetime far from the binary.

The direction of emission of linear momentum will rotate at frequency $\Omega(t)$, so the linear momentum emitted per unit time $\dot{\mathbf{P}}$ will have components

$$\dot{P}_x = f(t) \cos \phi(t) \quad \dot{P}_y = f(t) \sin \phi(t), \quad (1)$$

where ϕ is the time-changing angle in the orbital plane between the x axis and the direction in which linear momentum is being radiated.

The total linear momentum components carried away in the waves, from the start of emission at t_{start} to some particular time t , are the time integrals of \dot{P}_x and \dot{P}_y . Since $d\phi/dt$ will be always positive, $\phi(t)$ is an invertible function, and we can write the time integrals as

$$P_x = \int_{\phi(t_{\text{start}})}^{\phi(t)} \frac{f}{d\phi/dt} \cos \phi d\phi \quad P_y = \int_{\phi(t_{\text{start}})}^{\phi(t)} \frac{f}{d\phi/dt} \sin \phi d\phi. \quad (2)$$

We define $F(\phi) = f(t[\phi])/(d\phi/dt)$ and write the integrals in the suggestive form

$$P_x = \int_{\phi(t_{\text{start}})}^{\phi(t)} F(\phi) \cos \phi d\phi = F(\phi) \sin \phi + F' \cos \phi - F'' \sin \phi \pm \dots \Big|_{\phi(t_{\text{start}})}^{\phi(t)} \quad (3)$$

$$P_y = \int_{\phi(t_{\text{start}})}^{\phi(t)} F(\phi) \sin \phi d\phi = -F(\phi) \cos \phi + F' \sin \phi + F'' \cos \phi \pm \dots \Big|_{\phi(t_{\text{start}})}^{\phi(t)}. \quad (4)$$

Here $F' = dF/d\phi = \Omega^{-1}dF/dt$ and is of order $(T/\tau)F$, where τ is the timescale for change of F , and where $T = 2\pi/\Omega$ is the period of the oscillatory process.

For a slowly decaying binary there is a very small fractional change in f and Ω , and hence in F , over an orbit. We tentatively assume that this is true for any of the orbits before the plunge, and that it is also true in the late post-plunge epoch of the merger when Ω is to be interpreted as the frequency associated with the quasinormal ringing of the final black hole. In short, we tentatively assume that the ‘‘slowness parameter’’ T/τ is small throughout the integration. Thus $F \gg F' \gg F'' \gg \dots$, and for slowly changing orbits keeping only the first term on the right, or the first few terms, is a good approximation.

We now add the assumption that the strength of gravitational emission vanishes at the start of the binary inspiral. This is simply the statement that the starting separation is large enough that the early emission is tiny compared to the emission at the time of interest. From Eqs. (3) and (4) we then have that the total of the momentum radiated during the inspiral from t_{start} to t is

$$P_x(t) = \frac{f(t)}{\Omega(t)} \sin \phi(t) [1 + \mathcal{O}(T/\tau)] \quad P_y(t) = -\frac{f(t)}{\Omega(t)} \cos \phi(t) [1 + \mathcal{O}(T/\tau)]. \quad (5)$$

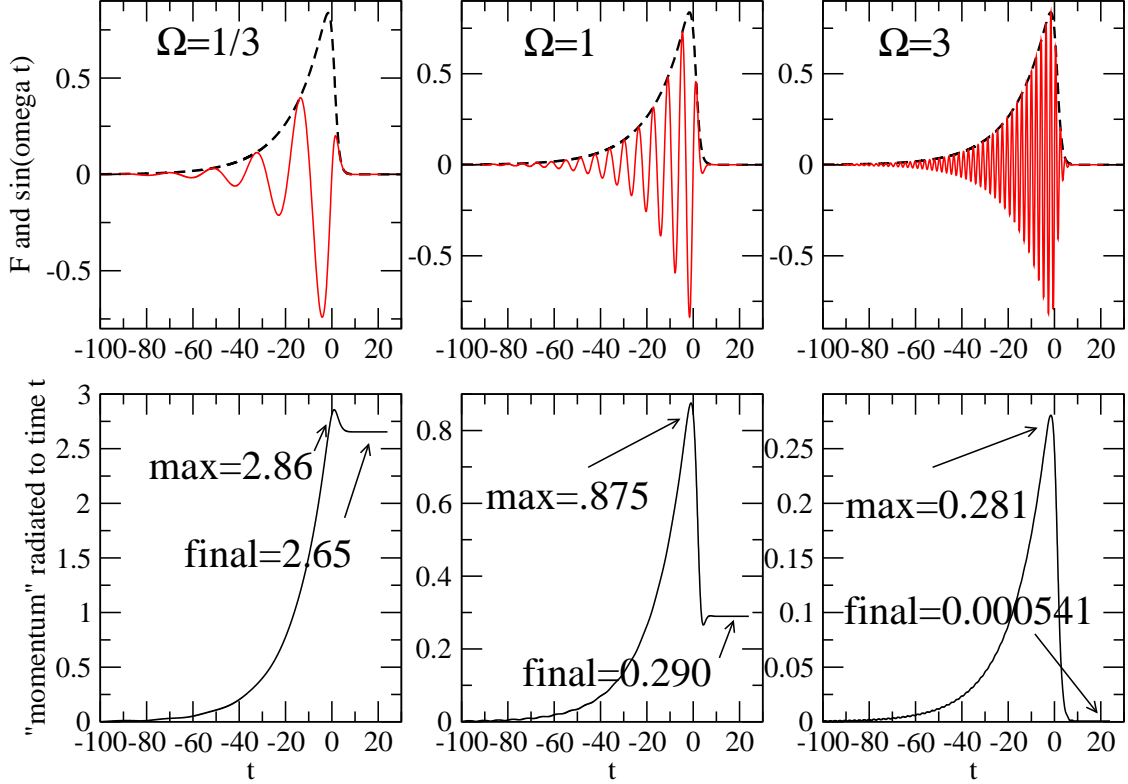


FIG. 1. The top row shows the envelope function $f(t)$ for our model problem and compares it with the oscillations $\sin(t/3)$, $\sin(t)$, and $\sin(3t)$. The second row shows the “momentum” radiated up to time t for models with the three different choices of Ω .

For the binary inspiral of two black holes, or of a black hole and a particle, the amplitude of gravitational wave emission increases slowly until the start of the “plunge” phase of inspiral. Around that time emission reaches a maximum, then decreases and dies out with the damped sinusoidal pattern of the quasinormal ringing of the final hole being formed. The epoch of plunge and quasinormal ringing is not typically characterized by values of T/τ as small as those in the slow inspiral, but in many cases, especially those involving rapidly rotating holes, the value of T/τ remains generally small (though this issue will be more closely examined below).

We separate the binary process into the epoch $-\infty < t < t_{\text{plunge}}$ before the smooth inspiral begins the inward plunge and the post-plunge epoch $t_{\text{plunge}} < t < \infty$. We tentatively assume that the same $T/\tau \ll 1$ approximation can be applied throughout the entire inspiral, plunge

and quasinormal ringing. Aside from corrections of fractional order $\mathcal{O}(T/\tau)$, we have then from Eq. (5) that the momentum emitted up to the time of plunge is

$$P_x = \frac{f(t_{\text{plunge}})}{\Omega(t_{\text{plunge}})} \sin \phi(t_{\text{plunge}}) \quad P_y = -\frac{f(t_{\text{plunge}})}{\Omega(t_{\text{plunge}})} \cos \phi(t_{\text{plunge}}). \quad (6)$$

Since f vanishes at $+\infty$ as well as $-\infty$, Eqs. (3),(4), with t_{start}, t replaced by $t_{\text{plunge}}, +\infty$ tell us that the post-plunge components are

$$P_x = -\frac{f(t_{\text{plunge}})}{\Omega(t_{\text{plunge}})} \sin \phi(t_{\text{plunge}}) \quad P_y = \frac{f(t_{\text{plunge}})}{\Omega(t_{\text{plunge}})} \cos \phi(t_{\text{plunge}}). \quad (7)$$

The conclusion is that the post-plunge emission cancels the pre-plunge emission, aside from corrections of order T/τ . It should be noted that t_{plunge} can be chosen to be any value of t , and so that our conclusion is that for a slow process the total momentum radiated is negligible. That conclusion is immediate if we put $-\infty, +\infty$ in place of t_{start}, t in the integrals in Eq. (5). With this substitution it can also be seen that the components of the total momentum emission are equivalent to the Fourier transform of the function $F(\phi)$ at “frequency” unity. In the case that $T/\tau \ll 1$, the function $F(\phi)$ changes little for $\Delta\phi = 2\pi$, and this Fourier component will be small. Somewhat loosely speaking, this is the statement that antikick cancels the kick to the extent that the rate of change of the emission is slow compared to the rate of orbiting, plunging and ringing.

Our analysis in Eqs. (6) and (7) is more than just the statement of negligible total radiation. If t_{plunge} is the time at which $f(t)/\Omega(t)$ is a maximum, then those equations imply that the momentum radiated up to time t_{plunge} is much larger than the momentum that remains after the cancelation. If the approximation $T/\tau \ll 1$ were strictly valid for $-\infty < t < \infty$, then the conclusion would be that the total momentum radiated is smaller than the maximum by a factor of order T/τ .

B. Examples

Before applying the above ideas to actual binary computations, it is useful to start with the definitiveness of a simple toy model. For the model to be simple we will choose Ω to be a constant, and will choose $f(t)$, the analog of the “intensity” of $|\dot{\mathbf{P}}|$ to be the function

$$f(t) = \frac{e^{t/15}}{1 + e^{t-1}}. \quad (8)$$

This function, shown as the dashed curve in the top row of the panels in Fig. 1, plays the role of the envelope of the oscillations of \dot{P}_x and \dot{P}_y . The particular choice in Eq. (8) has some flavor of the actual envelope of the momentum oscillations for a binary inspiral. It starts slow, at large negative times, with $f(t) \approx e^{t/15}$, and finishes at a more rapid pace, with $f(t) \propto e^{-14t/15}$. We can take the timescale for change to be $\tau = |f/(df/dt)|$. This timescale starts at 15 at large negative times, diverges at around $t = -1.64$ and approaches a magnitude 15/14 at large positive times. For this simple envelope the minimum timescale is therefore 15/14.

The analog of \dot{P}_y is $f(t) \sin \Omega t$ where Ω is the orbital/ringing frequency (constant for our toy model). We consider three possible values $\Omega = 1/3, 1, \text{ or } 3$. (With a simple rescaling $t' = \Omega t$ this is equivalent to the choice of a single orbital/ringing frequency and three different “slownesses” of the envelope function $f(t)$.) With periods $T = 6\pi, 2\pi, 2\pi/3$, the slowness parameter T/τ in each case has a maximum of 17.6, 5.86, and 1.95, respectively. In the top row of Fig. 1 the envelope is shown along with the sinusoidal oscillations. It clear that these numerical indicators are compatible with the visual appearance of the curves. For $\Omega = 1/3$, the envelope (at large time) changes more rapidly than the oscillations; for $\Omega = 1$ the envelope and oscillations change at a comparable rate; for $\Omega = 3$ the envelope changes more slowly than the very rapid oscillations.

The “momentum” radiated in the toy model has been computed for each of the three cases. That is, the following integrals have been computed

$$P_x(t) = \int_{-\infty}^t \frac{e^{t'/15} \sin \Omega t'}{1 + e^{t'-1}} dt' \quad P_y(t) = \int_{-\infty}^t \frac{e^{t'/15} \cos \Omega t'}{1 + e^{t'-1}} dt'. \quad (9)$$

The results for the total momentum radiated $\sqrt{P_x^2 + P_y^2}$, as a function of time, are shown in the second row of of Fig. 1. In the case of the truly slow envelope, with $\Omega = 3$, the “kick” (maximum of the momentum radiated) is 0.281, while the final value .000541 is only 0.2% of the maximum kick. The post-“plunge” antikick has canceled 99.8% of the pre-“plunge” maximum. The remaining cases, for $\Omega = 1$ and $1/3$, show that there is a clear correlation of the slowness and the extent to which the antikick cancels the kick. They also show that while the correlation is strong, it is not simple. The ratios of final momentum to maximum momentum is 0.93, 0.33, 0.0019 for $\Omega = 1/3, 1, 3$ respectively. This is a much more dramatic dependence on slowness than the ratios of the timescales.

We now look at similar considerations for actual particle perturbation models. We start

with the results that were used in Ref. [11], and that correspond to a very small mass ratio (particle mass to black hole mass) $\mu = 10^{-4}$, and hence to a very slow early pre-plunge epoch, when inspiral is driven by the loss of orbital energy to gravitational waves. The plots in the top row of Fig. 2 show \dot{P}_x as a function of time. The particular values of t/M have no absolute meaning, so we have translated the results here, and in subsequent plots, so that $t/M = 0$ always corresponds to the time of maximum radiated momentum.

At early time these oscillations are characteristic of the rotation of the system. (In this particle perturbation model it is the rotation of the particle in the Kerr background.) The intensity of the gravitational radiation increases until the system reaches its smallest stable separation, at around time $t/M = 0$. This point of maximum emission roughly signals the start of the plunge as the particle goes inside the radius for the innermost stable circular orbit. The subsequent radiation pattern, within an oscillation or two, becomes that of quasinormal ringing.

A striking feature of Fig. 2 is that the frequency for the pre-plunge momentum oscillations for $a/M = 0.9$ is significantly higher than for $a/M = 0.6$. This is due to the fact that the radius of innermost stable circular orbit, the “ISCO” in the Kerr spacetime, is a decreasing function of a/M , and the angular frequency for the innermost orbit is an increasing function of a/M [11]. The period of the oscillations as the plunge is approached are in agreement with the analytically known frequencies at the ISCO. It is tempting to infer that this higher pre-plunge frequency for $a/M = 0.9$ as compared with $a/M = 0.6$ accounts for the greater antikick cancellation of the kick, just as the toy model with $\Omega = 3$ exhibited greater antikick cancellation than did the smaller values of Ω . We will argue that this temptation should be resisted.

Figure 3 shows the results for mass ratio $\mu = 10^{-2}$ that correspond to the results for $\mu = 10^{-4}$ in Fig. 2. The most notable difference in the momentum generation in the two cases is that the pre-plunge evolution of the envelope is significantly faster for $\mu = 10^{-2}$ than it is for $\mu = 10^{-4}$. If the antikick cancellation depended on how gradually the envelope of oscillations changes prior to the plunge then we would expect that the $\mu = 10^{-2}$ results would exhibit weaker antikick cancellation than the $\mu = 10^{-4}$ results. This turns out not to be the case; the fraction of the kick cancelled is roughly the same for the two values of μ . The computed cancellation for these models, and also for $a/M = 0.7$ and $a/M = 0.8$, are shown in Table I.

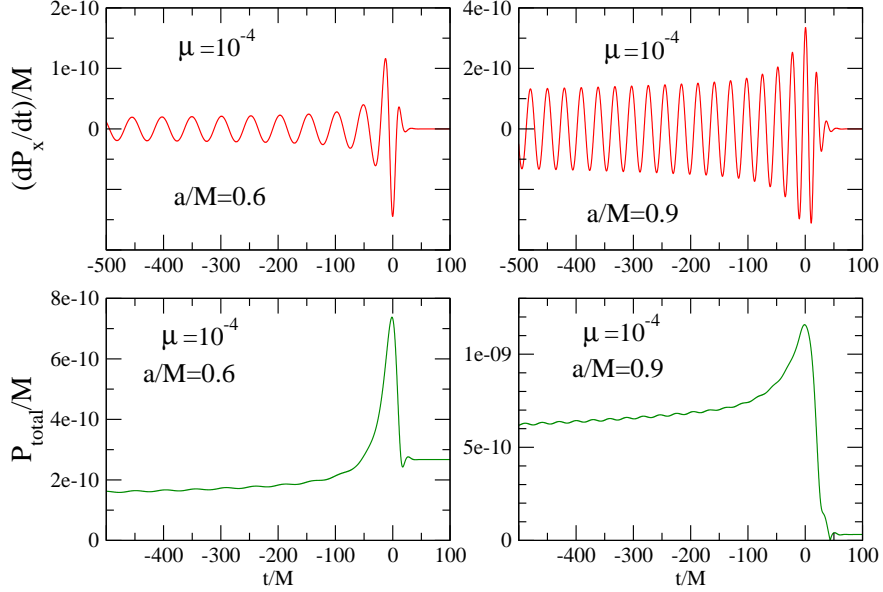


FIG. 2. Computational results for mass ratio $\mu = 10^{-4}$ in the case of black hole spin parameters $a/M = 0.6$ and $a/M = 0.9$.

	mass ratio $\mu = 10^{-2}$			mass ratio $\mu = 10^{-4}$		
a/M	P_{\max}	P_{final}	cancelled	P_{\max}	P_{final}	cancelled
0.6	5.37×10^{-6}	2.03×10^{-6}	62%	7.4×10^{-10}	2.7×10^{-10}	64%
0.7	5.57×10^{-6}	1.61×10^{-6}	71%	8.3×10^{-10}	2.0×10^{-10}	76%
0.8	6.46×10^{-6}	5.92×10^{-7}	91%	9.5×10^{-10}	1.1×10^{-10}	88%
0.9	6.48×10^{-6}	4.36×10^{-7}	93%	1.2×10^{-9}	3.2×10^{-11}	97%

TABLE I. Momentum results for models with mass ratios $\mu = 10^{-2}$ and $\mu = 10^{-4}$. The values of P_{\max} and P_{final} are the maximum and final value of the momentum radiated. The cancelled column, $1 - (P_{\text{final}}/P_{\max})$, is the fraction of the maximum kick that is cancelled by the later antikick.

Particle perturbation theory tells us that the amount of energy radiated during the pre-plunge inspiral, divided by the background mass, scales as μ . This is approximately confirmed by the results in Table I. The confirmation is only approximate because the nature of the onset of plunge is determined by the join of the quasicircular inspiral and the plunge, which represents dynamics that does not scale with the same μ factor as the early inspiral. What is particularly noteworthy is that the fraction of kick canceled by the antikick is rather insensitive to μ , and hence insensitive to how slow the early inspiral is.

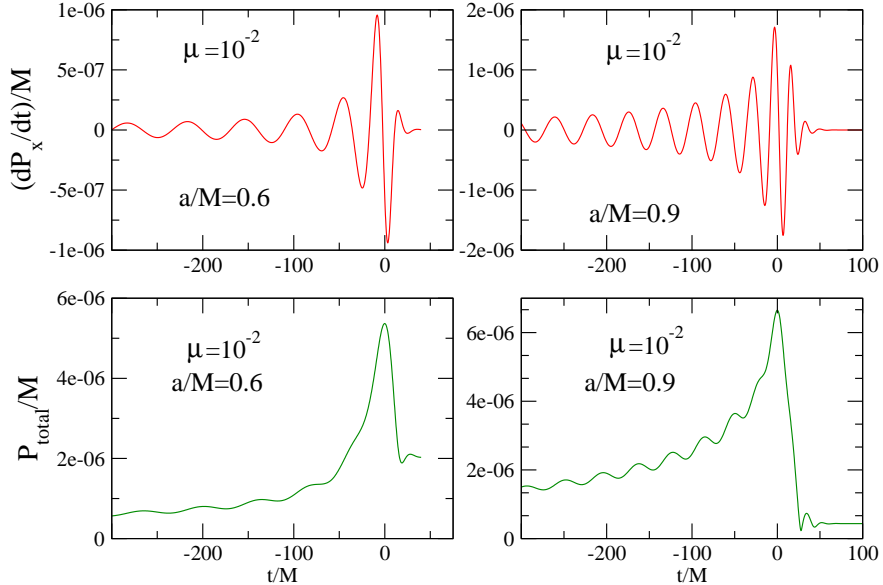


FIG. 3. Computational results for mass ratio $\mu = 10^{-2}$ in the case of spin parameters $a/M = 0.6$ and $a/M = 0.9$.

C. Implications of the results

If it is not the rate of change in the early slow inspiral that governs the size of the antickick, then what *does* govern it? The alternative explanation is the steepness of the post-plunge envelope. That is, the antickick cancellation of a large fraction of the kick depends on the extent to which the post-plunge envelope obeys the slowness condition. To test this explanation we return to the toy model of Eq. (8), but in the form

$$f(t) = \frac{e^{t/\tau_1}}{1 + e^{(t-1)/\tau_2}}, \quad (10)$$

with an adjustable early timescale τ_1 and late timescale $\tau_2/[1 - (\tau_2/\tau_1)]$. For this envelope function, we compute the “momentum” using the same integrals as in Eq. (9). Table II gives the results of the peak and final “momentum” for $\Omega = 1$. What is immediately striking about the results is that changes in the early slow timescale do not have a large effect on either the peak momentum or the final momentum, and that this is true for both values of the late fast timescale. A change in the late fast timescale, however, has a strong effect on the cancellation.

It is not “early” and “late” that are relevant here. (This is obvious in the fact that the momentum integrations can be run backwards in time[15].) What is relevant is that making

	$\tau_2 = 1$			$\tau_2 = 2$		
τ_1	P_{\max}	P_{final}	cancelled	P_{\max}	P_{final}	cancelled
5	0.842	0.332	61%	0.671	0.0287	95.7%
10	0.854	0.301	65%	0.698	0.0259	96.3%
15	0.875	0.291	67%	0.743	0.0251	96.6%
30	0.914	0.281	69%	0.821	0.0243	97.0%

TABLE II. Momentum results for the toy model with the envelope function defined in Eq. (10), and with $\Omega = 1$.

the slow process slower has little effect; making the fast process slower has a strong effect. In the context of binary inspiral/merger this means that it is the plunge and quasinormal ringing that are crucial to determining the impact of the antikick cancellation. This insight is potentially useful in numerical relativity modeling. It suggests that lessons learned from the very late epoch of modeling are what is important to cancellation, and that models can be started very late.

This insight about the impact of the speed of the late time process has implications also for understanding the qualitative roots of kick-antikick cancellation. For particle perturbation computations of radiated linear momentum reported in Ref. [11], the strength of the antikick is a rapidly increasing function of a/M . As exhibited in Fig. 5 of Ref. [11], the antikick is very small for $a/M = -0.3$, and negligible for $a/M = -0.6$ and -0.9 . (Negative values here indicate that the particle orbit is retrograde.) The patterns of momentum generation indicate that with a decrease of a/M , the momentum generation cuts off more quickly at the start of plunge. A plausible speculation is that this more rapid cut off is related to the larger ISCO for smaller a/M .

In the case of the inspiral/merger of comparable mass holes there is evidence in Fig. 15 of Schnittman et al.[9] that the correlations noted in particle perturbation models also apply. In particular, the antikick is most pronounced in the model in which the more massive hole has spin aligned with the orbital angular momentum. Though there is no strict meaning to an ISCO for binaries of comparable mass holes, this alignment of spins should play a role similar to that in EMRIs in governing the onset of the plunge-like epoch.

It is clear that the antikick cancellation is closely connected with how gradually the

intensity and period of momentum change. It is natural, therefore, to seek a quantification of the “slowness” of the momentum generation. The slowness is a function of time due to the intensity of the momentum generation ($f(t)$ of Eq. (1)) and the period ($T = 2\pi/\Omega(t)$). These are simple functions of time both in the early gradual inspiral and in the late quasinormal ringing, but cannot be simply characterized during the plunge. The period is particularly difficult to pin down during the plunge, since the plunge – the transition from quasicircular orbits to quasinormal ringing – typically takes only one oscillation, at least in the most interesting cases, the particle perturbation models with large positive a/M . As an indication of the difficulty of quantifying slowness we have therefore used the timescale for change in the envelope of the momentum oscillations $\tau = (d \ln f/dt)^{-1}$. To get the period as a function of time, a simple analytic fit was made to the period for a few cycles before and after the plunge (i.e., the peak of emission). Figure 4 shows the results for the slowest case, that of $a/M = 0.9$, the case for which slowness should be most easily quantified. The figure shows that the early inspiral is “slow” by this criterion. (The period is much shorter than

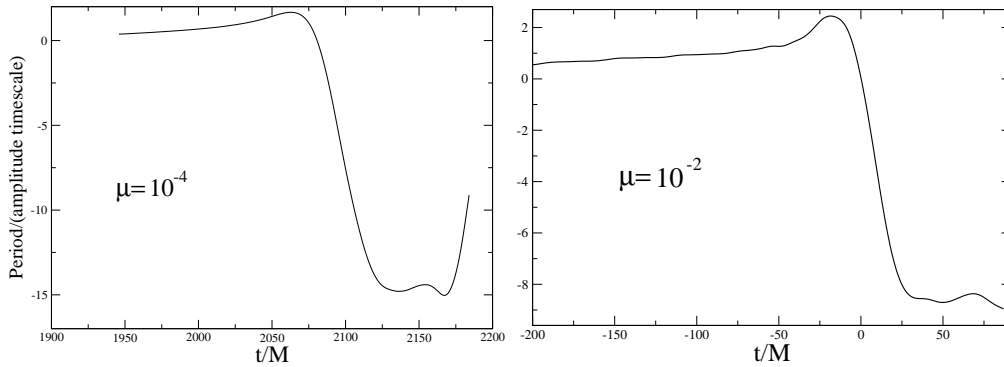


FIG. 4. An indicator of “slowness,” the ratio of the oscillation period to the timescale for change in the strength of the momentum emission, for the particle-perturbation models with $a/M = 0.9$ both for $\mu = 10^{-4}$ and $\mu = 10^{-2}$.

the timescale for change.) As the process approaches the plunge, it becomes faster, but still satisfies the criterion of being reasonably slow. However, at the plunge (interpreted here as the steep descent of the curves in Fig. 4) the process seems badly to violate the slowness criterion. Though the slowness approximation explanation for the systematics of the cancellation appears to give an excellent accounting of all results, we see that it is not strictly valid. The success can be understood, at least partially, from the fact that when

the slowness approximation fails, the rate of generation of momentum has already greatly decreased.

It would of course be useful, or at least satisfying, to have a quantification of slowness that is more meaningful than that exhibited in Fig. 4, but this is probably not possible, as had already been suggested by Damour and Gopakumar[10]. The greatest challenge is that a quantification requires that we characterize the frequency through the plunge. For Fig. 4 we have used the crude method of noting zero crossings and fitting a simple function for $\Omega(t)$. Much more sophisticated methods exist for separating changes into those of amplitude and frequency, such as the normalized Hilbert transform[16], but no method can effect such a separation in the case that the period is comparable to the timescale for change. A more promising approach may be a semianalytic joining of the quasicircular inspiral to the quasinormal ringing rooted in modeling of the EMRI or comparable mass processes.

III. THE SLOWNESS APPROXIMATION AS AN AID TO MODEL COMPUTATIONS

The analysis of the previous section can be used to reduce the computational burden in running models, both with the particle perturbation approximation, and with fully nonlinear gravity. The underlying principle is that the slowness approximation is highly justified in the very early stages of inspiral. By exploiting the slowness approximation we can eliminate the need to carry out model computations from very early times; models can be run starting at relatively late times. Here we focus on using the approximation for momentum computations.

A. The $1/\Omega$ approximation

The fundamental idea in using the slow approximation to replace early orbits is to use the approximations in Eq. (5), ignoring the corrections of order T/τ . With corrections ignored, Eqs. (1) and (5) give us

$$P_x(t) = \dot{P}_y(t)/\Omega(t) \quad P_y(t) = -\dot{P}_x(t)/\Omega(t). \quad (11)$$

To illustrate the validity of this approximation we choose the example $\mu = 10^{-2}$ and $a/M = 0.6$. For the slow approximation this should be the most severe test, since the low mass ratio

and the moderate value of a/M both favor fast changes.

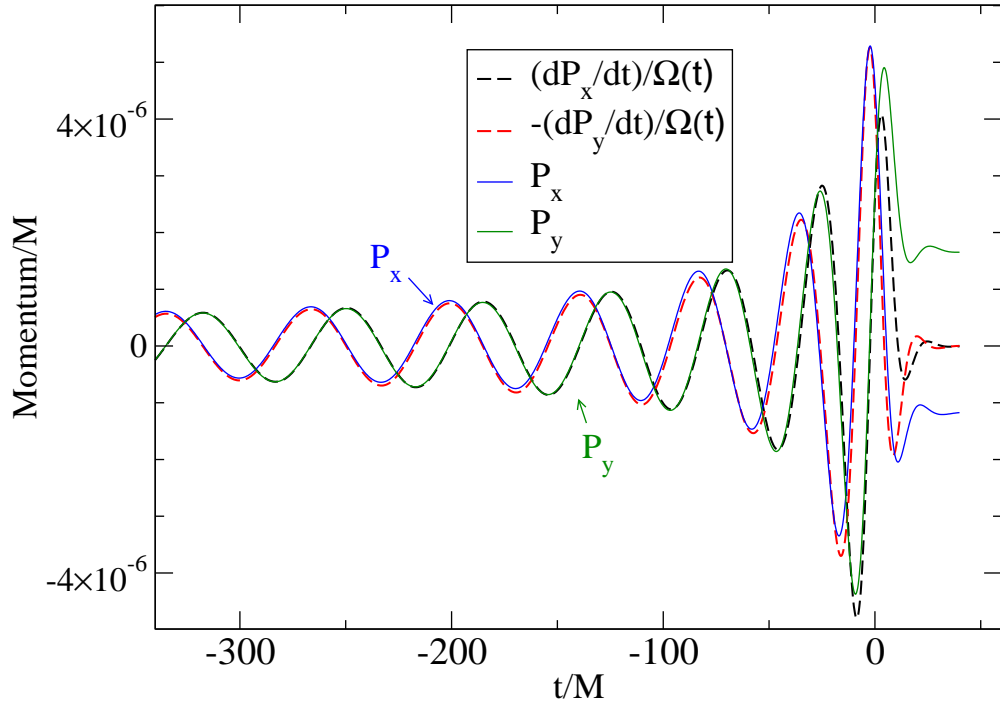


FIG. 5. Momentum radiated during inspiral for a model with $\mu = 10^{-2}$, $a/M = 0.6$. The solid curves are the computed momenta as a function of time. The dashed curves are the approximation according to Eq. (11).

Figure 5 shows that even for this case the success of the slow approximation is remarkable. The figure shows the comparison of the two sides of each of the equalities in Eq. (11). We see that before the plunge $P_x(t)$ is almost indistinguishable from $\dot{P}_y(t)/\Omega(t)$ and $P_y(t)$ is almost indistinguishable from $-\dot{P}_x(t)/\Omega(t)$. The momentum values, and their slow approximation values, begin to deviate noticeably only around $t/M = 20$, only slightly earlier than the nominal start of plunge at $t/M = 0$.

The usefulness of this approximation is clear. If we want to compute the momentum radiated during an inspiral, we need not start at a time long before the plunge. In fact, we need only start early enough so that the inevitable numerical noise from the starting process has subsided by the time the model is within a single oscillation of the plunge!

B. Integration from a local peak

We now describe a technique for finding the value of P_x that requires only the computation of \dot{P}_x (and similarly for P_y). In this approach we note that $P_x = 0$ at a value of t/M at which $\dot{P}_y = 0$. To the same order in the approximation, it is a time at which $|\dot{P}_x|$ is a maximum. This means that we will get results that are accurate to the order of the approximation if we start integrating for P_x , with P_x set to zero, at a time when \dot{P}_x is a maximum, i.e., at a local peak. An appropriately modified version of this statement applies for the computation of P_y .

In Fig. 6 we show the results of this method used to compute the radiated momentum for the model with $\mu = 10^{-2}$ and $a/M = 0.8$. The curves give results for integration starting at different epochs. Since the peak of the rate of emission occurs around $t/M = 0$, it is rather remarkable that integration starting as late as $t/M = -100$, gives results that are the same, within the accuracy of the modeling, with integration started around $t/M = -700$.

IV. CONCLUSIONS

The explanations and approximations in the previous section can be considered to be based on understanding the inspiral radiation for circular, equatorial binary inspiral with a model that is rooted in the idea of a rotating beam of radiated momentum, whether in a particle perturbation computation or in numerical relativity computations with the fully nonlinear theory. For radiated momentum confined to the orbital plane we have shown that an explanation of the kick/antikick cancellation follows from treating the change in the amplitude and frequency of the momentum components as slow compared to the period of the oscillations.

In the early quasicircular inspiral, this slowness approximation is rigorously true and leads to efficient methods for starting a computation at late times, just before the plunge, while getting an accurate value of the momentum radiated since the start of inspiral.

We have argued that no simple prescription exists for characterizing the momentum during the plunge. Damour and Gopakumar[10], arguing similarly, pointed out that this prevented an accurate estimate of radiated momentum based on the effective one body approach.

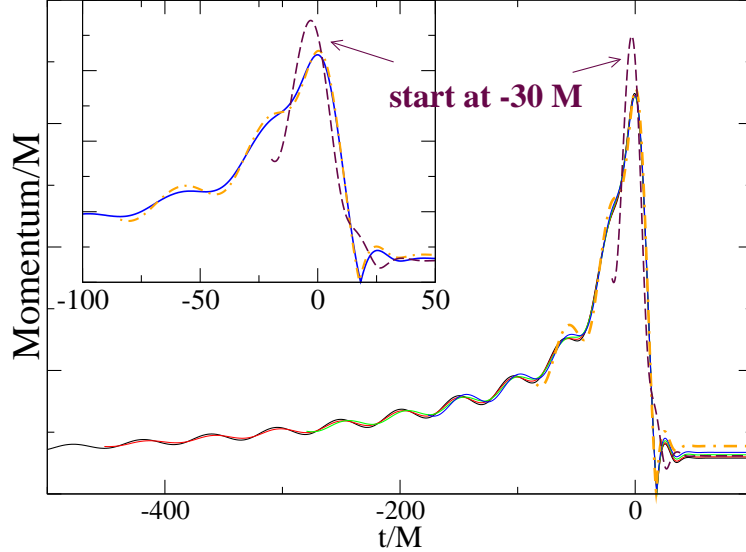


FIG. 6. Momentum computed, as a function of time, using integration from the peak. For models with $\mu = 10^{-2}$, $a/M = 0.8$, results are shown for the total momentum computed using integration of P_x starting from a maximum of \dot{P}_x , and similarly for P_y . Plots are included starting approximately at times $-700M$, $-500M$, $-300M$, $-200M$, $-100M$ and $-30M$. The curve for integration started at $-100M$ has dots and dashes; the curve for integration started at $-30M$ is shown with long dashes. Remarkably, even the $-100M$ curve, starting very near the plunge, gives a good approximation for the momentum.

Though a simple prescription is ruled out, it is plausible that a study of the plunge dynamics will provide guidelines that allow explanations and approximations for antikick cancellations. This is very likely in the particle perturbation approach, in which the plunge dynamics is governed by orbits in the Kerr background. The lessons learned from particle perturbation models may lead to a better understanding, or categorization of the antikick for the inspiral/merger of comparable mass holes.

Most of the insights and methods above are specific to the case of inspiral/merger in which the momentum is confined to the orbital plane. The general inspiral/merger, however, will not have this equatorial symmetry. In the case of a particle perturbation model, the particle orbit will be inclined to the equatorial plane and there will be a component of radiation in the z direction (parallel to the hole angular momentum) as well as in the orbital xy plane. The simple fit to an oscillation (with a time changing frequency) will not suffice, since at

any epoch there will be a motion in the z direction as well as in the x and y directions. There will then be two time varying frequencies, each with its time varying amplitude. It is interesting to ask whether there are any insights or results in such cases analogous to those for the simple equatorial case.

Initial numerical experiments suggest that it is possible to fit the late pre-plunge inspiral to a two frequency model, at least in the case that of particle perturbation results with only a small tilt out of the equatorial plane. We intend to pursue this idea for nonequatorial orbits both with particle perturbation results and with results from numerical relativity. Of particular interest is an objective procedure in which the two nonconstant frequencies are extracted from the late pre-plunge data using the Hilbert-Huang transformation [16] a technique that is ideally suited to extract sets of modes that have different, nonconstant frequencies.

ACKNOWLEDGMENTS

RHP gratefully acknowledges support of this work by NSF Grant 0554367, and from the UTB Center for Gravitational Wave Astronomy. This work was supported at MIT by NASA Grant No. NNG05G105G and NSF Grant PHY-0449884. GK acknowledges research support from NSF Grants PHY-0902026, CNS-0959382 and PHY-1016906, and hardware donations from Sony and IBM. Some of the data presented in this work was generated on the Air Force Research Laboratory CONDOR supercomputer. GK acknowledges support from AFRL under CRADA No. 10-RI-CRADA-09.

-
- [1] F. Pretorius, Physical Review Letters **95**, 121101 (2005), arXiv:gr-qc/0507014.
 - [2] M. Campanelli, C. O. Lousto, P. Marronetti, and Y. Zlochower, Physical Review Letters **96**, 111101 (2006), arXiv:gr-qc/0511048.
 - [3] J. G. Baker, J. Centrella, D. Choi, M. Koppitz, and J. van Meter, Physical Review Letters **96**, 111102 (2006), arXiv:gr-qc/0511103.
 - [4] M. Volonteri, K. Gültekin, and M. Dotti, Mon. Not. R. Astron. Soc. **404**, 2143 (2010); also arxiv:1001.1743

- [5] O. Zanotti, L. Rezzolla, L. Del Zanna, and C. Palenzuela, *Astron. and Astrophys.* **523**, A8 (2010); also arxiv:1002.4185.
- [6] J. Guedes, P. Madau, L. Mayer, and S. Callegari, *Astrophys. J.* **729**, 125 (2011); also arxiv:1008.2032.
- [7] D. Sijacki, V. Springel, and M. Haehnelt, *Mon. Not. R. Astron. Soc.*, submitted; also arxiv:1008.3313.
- [8] L. Blecha, T. J. Cox, A. Loeb, and L. Hernquist, *Mon. Not. R. Astron. Soc.*, in press; also arxiv:1009.4940.
- [9] J. D. Schnittman, A. Buonanno, J. R. van Meter, J. G. Baker, W. D. Boggs, J. Centrella, B. J. Kelly, and S. T. McWilliams, *Phys. Rev. D* **77**, 044031 (2008), 0707.0301.
- [10] T. Damour and A. Gopakumar, *Phys. Rev. D* **73**, 124006 (2006), arXiv:gr-qc/0602117.
- [11] P. A. Sundararajan, G. Khanna, and S. A. Hughes, *Phys. Rev. D* **81**, 104009 (2010), 1003.0485.
- [12] Y. Mino and J. Brink, *Phys. Rev. D* **78**, 124015 (2008), 0809.2814.
- [13] In Eq. (5.2) of Ref. [11] the reported maximum recoil for this case contains a misprint. The actual value of v^{peak}/c is $0.12(\mu/M)^2$ rather than $0.17(\mu/M)^2$. The value of v^{peak}/c shown in Fig. 5 of that paper is correct.
- [14] L. Rezzolla, R. P. Macedo, and J. L. Jaramillo, *Physical Review Letters* **104**, 221101 (2010), 1003.0873.
- [15] The time reversal also requires, in principle, additions to the momentum so that the $t = \infty$ value of P_x, P_y are zero.
- [16] N. Huang and S. Shen, *Hilbert Huang Transform and Its Applications* (World Scientific, 2005).